COMMUNICATIONS CHEMISTRY

ARTICLE

DOI: 10.1038/s42004-017-0003-x OPEN

Visible chiral discrimination via macroscopic selective assembly

Yongtai Zheng [1,2], Yuichiro Kobayashi [1,2], Tomoko Sekine[1,2], Yoshinori Takashima [3], Akihito Hashidzume [3], Hiroyasu Yamaguchi[3] & Akira Harada[1,2]

The transfer of chirality from individual molecules to macroscopic objects, and the recognition of chirality on the macroscopic scale have potential for many practical applications, but they are still key challenges for the chiral research community. Here we present a strategy for visible chiral recognition by macroscopic assembly using polyacrylamide-based gels modified with β-cyclodextrin (βCD-gel) and D- or L-tryptophan (homochiral D- or L-Trp-gel), which differs from most methods reported, e.g., colorimetric or chromogenic methods, fluorescence, gel formation and collapse. The circular dichroism spectra demonstrate that the chirality of Trp molecules is successfully transferred and amplified in the corresponding Trp-gels. The chirality of the D- and L-Trp-gels is macroscopically recognized by the βCD-gel selectivity in aqueous NaCl through the amplification of interfacial enantioselective host–guest interactions.

[1] Project Research Center for Fundamental Sciences, Graduate School of Science, Osaka University, Toyonaka, Osaka 560-0043, Japan. [2] JST-ImPACT, 5-7, Chiyoda-ku, Tokyo 100-8914, Japan. [3] Department of Macromolecular Science, Graduate School of Science, Osaka University, Toyonaka, Osaka 560-0043, Japan. Correspondence and requests for materials should be addressed to A.H. (email: harada@chem.sci.osaka-u.ac.jp)

Chirality is widely regarded as a biosignature and vital to living organisms at both the microscopic and macroscopic levels[1]. For example, proteins are formed from L-amino acids, whereas nucleic acids contain D-sugars such as D-deoxyribose or D-ribose. The biomacromolecules further organize to form cells and tissues to generate asymmetric conformations and physical properties on a macroscopic scale, e.g., the spiral structure of shells, cucumber tendrils, and asymmetric appendages of organisms; differences in optical activities, tastes, and smells for a pair of enantiomers[2].

Although chirality transfer and chiral recognition from the microscopic to the macroscopic scale have promise for many practical applications, e.g., chiral separation[3–5], optical memories and switches[6–9], and functional sensors and actuators[10–13], they still remain key challenges in artificial systems[1,2,14]. To scale up chirality, a supramolecular strategy is generally employed to obtain various chiral architectures via assemblies of chiral or achiral molecules through non-covalent interactions[15–17]. Another strategy is a polymeric method, in which rigid main-chain or chiral units appear as helical structures with exclusive handedness[18–20]. The local chiral signals of monomeric molecules are primarily transformed to conformational chiral information during chirality transfer[15,21,22], and this information could be switchable instead of being permanent[23–25], although preserving uniformity for local and global chirality is desirable for better understanding chiral amplification and recognition. Moreover, significant effort has been put into achieving visible observation of chiral recognition and discrimination on the macroscopic scale. Strategies include colorimetric or chromogenic methods[26–28], fluorescence[29–31], crystal morphology[32,33], gel formation and collapse[34–36], and wettability switching[37–39]. By contrast, simultaneously observing chiral discrimination via side-by-side comparison of a pair of enantiomers, as clearly as we distinguish our left and right hands, has rarely been reported.

Cyclodextrins, cyclic oligomers of D-glucopyranose units with a conical chiral cavity, have chirality sensing ability through host–guest interactions[40–42]. Consequently, cyclodextrins are employed in various matrixes for applicable enantiomeric selectivity and separation, e.g., microspheres, nanochannels, electrodes, and the stationary phase of columns[43–46]. Additionally, L-tryptophan (L-Trp) is an essential amino acid for the composition of proteins, whereas D-Trp has probiotic properties that can stimulate the immune system[47]. Trp molecules can be incorporated into β-cyclodextrins (βCD) or complexed with metals such as Pt(II) and Cu(I) owing to their high hydrophobicity and electron density[48]. βCD shows a slight chiral preference toward L-Trp over D-Trp due to steric hydrogen bonding during inclusion complex formation[45,49,50].

On the basis of our previous studies of macroscopic molecular recognition[51–59], herein we show visible macroscopic chiral recognition that relies on interfacial enantioselective host–guest interactions. The chiral signals of the D- or L-Trp residues are seeded into poly(acrylamide) (pAAm)-based hydrogels (D- or L-Trp(x)-gels), in which the chirality is successfully transferred and amplified to the macroscopic scale. The interactions between the pAAm-gel bearing βCD moieties (βCD-gel) and the D-Trp(x)-gel and L-Trp(x)-gel are investigated in aqueous solutions with different components. Under appropriate conditions, such as in aqueous NaCl, the βCD-gel can successfully discriminate the D-Trp(x)-gel from L-Trp(x)-gel on a macroscopic scale by amplifying enantioselective host–guest recognition through interfacial multisite interactions.

Results

Synthesis and characterization of gels. Acrylamido D- or L-Trp (AC-Trp(D or L)) monomer was prepared from BOC (*tert*-butoxycarbonyl) protected BOC-Trp(D or L) in three steps

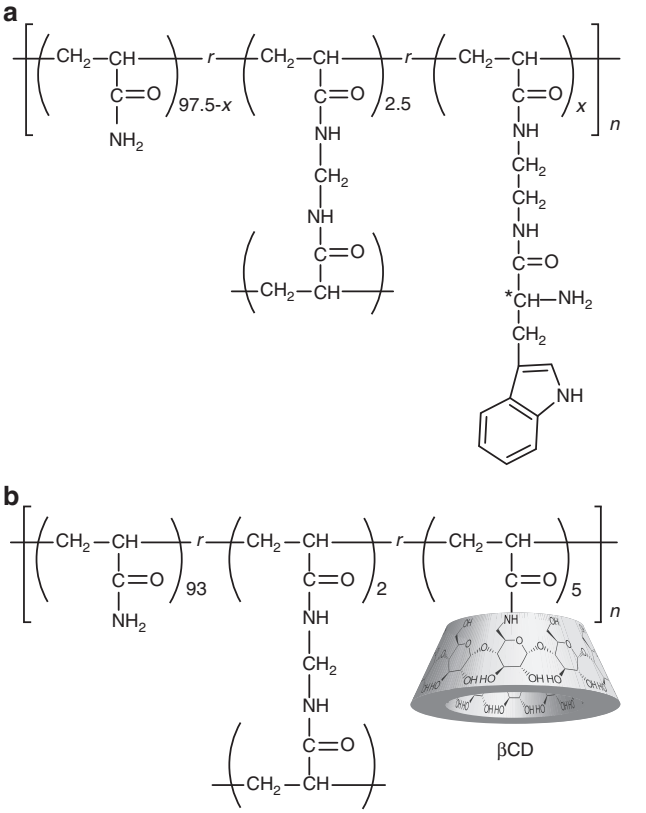

Fig. 1 Chemical structures of homochiral tryptophan and β-cyclodextrin gels. **a** Homochiral D- or L-Trp(x)-gel, where x denotes the mol% of Trp monomers in the reaction mixture. **b** βCD-gel. The βCD monomer is fixed at 5 mol%

(Supplementary Fig. 1–3). Homochiral D- or L-Trp(x)-gel (x denotes the mol% of AC-Trp(D or L) in the reaction mixture) was then prepared from the radical terpolymerization of acrylamide (AAm), *N*,*N*′-methylenebis(acrylamide) (MBA), and AC-Trp(D or L) monomers in DMSO using Irgacure 184 as the initiator under UV light at room temperature (Fig. 1). The resulting gels were washed with DMSO and immersed in excess water or 0.9 wt % aqueous NaCl (NaCl aq.). The βCD-gel was prepared according to our previous report[56]. Predetermined amounts of AAm, MBA, and mono(6-deoxyacrylamido)-β-cyclodextrin (5 mol%) were terpolymerized in water at room temperature using APS (ammonium persulfate) and TMEDA (tetramethylethylenediamine) as the initiator. The obtained βCD-gel was washed with water and immersed in excess of water or NaCl aq.

The chemical compositions for the D-Trp(x)-gel, L-Trp(x)-gel, and βCD-gel were determined by ^{1}H FG-MAS-NMR, for which the ratios for each residue were practically the same as those in reaction mixture (Supplementary Fig. 4 and 5).

Gel swell-shrink properties in various aqueous solutions. The swelling properties of the D-Trp(x)-gel, L-Trp(x)-gel, and βCD-gel were observed and recorded after immersion in pure water, NaCl aq., or 10 mM aqueous Na_2PdCl_4 (Pd(II) aq.) for 3 days. Their swelling ratios (V/V_0) and corresponding concentrations are illustrated in Fig. 2 (Supplementary Table 1).

D-Trp(x)-gel and L-Trp(x)-gel were as-synthesized from DMSO and expanded substantially after exchanging solvent molecules for water molecules (~24 and 31 times for $x = 3$ and 5,

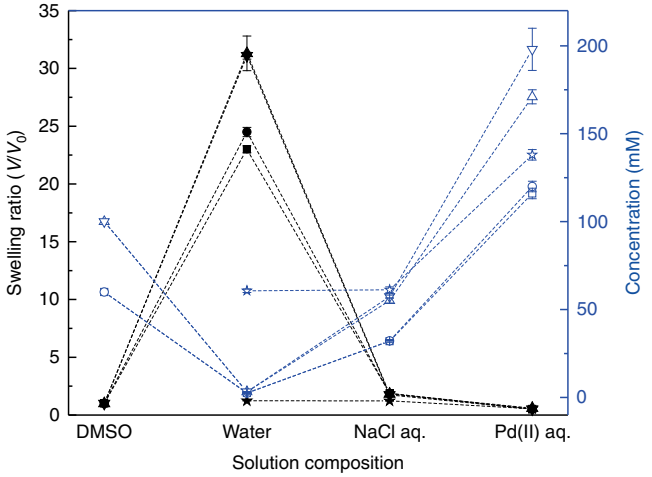

Fig. 2 Swelling ratios and corresponding concentrations for the gels in different solutions. Swelling ratios and corresponding concentrations for the D-Trp(3)-gel (solid and open squares), L-Trp(3)-gel (solid and open circles), the D-Trp(5)-gel (solid and open triangles), the L-Trp(5)-gel (solid and open inverted triangles), and the βCD-gel (solid and open stars). NaCl aq. and Pd (II) aq. represent 0.9 wt% NaCl and 10 mM Na_2PdCl_4 aqueous solution, respectively. Both D- and L-Trp(*x*)-gels were extraordinarily swollen in pure water, they slightly expanded in NaCl aq., and they shrank in Pd(II) aq. The concentrations are inversely related to swelling. The βCD-gel was only swollen a small amount in water and NaCl aq. but did shrink in Pd(II) aq. See Supplementary Table 1 for specific numerical values. Error bars show the standard deviation of measurements for three samples

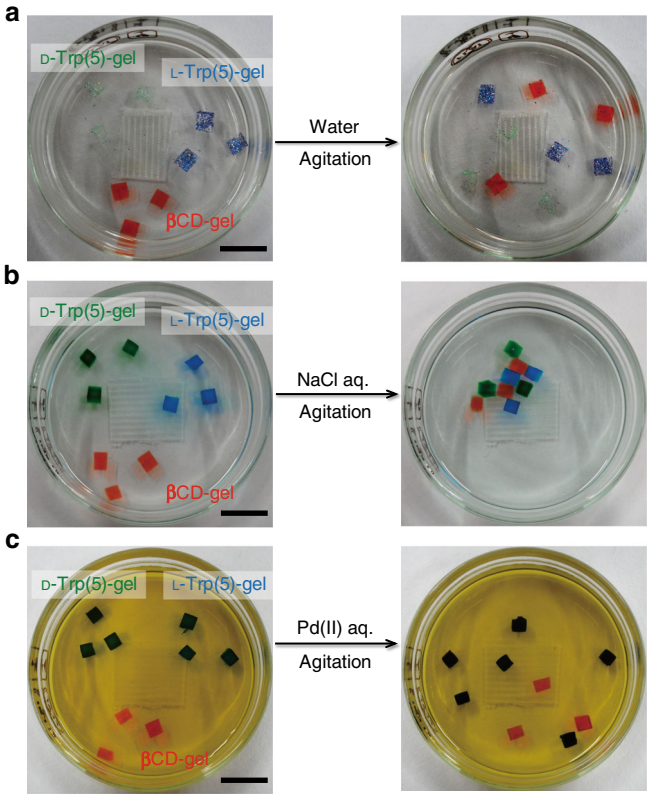

Fig. 3 Pictures of solvent effects on molecular recognition between gels. **a** No interaction between the D- and L-Trp(5)-gels with the βCD-gel was observed in water. **b** The βCD-gel assembled with both the D- and L-Trp(5)-gels in NaCl aq. **c** No interaction between the D- and L-Trp(5)-gels with the βCD-gel was observed in Pd(II) aq. Scale bars, 1.0 cm

respectively, Supplementary Fig. 6). Accordingly, both D- and L-Trp(*x*)-gels become particularly fragile due to dramatic expansion. This finding greatly differs from that of our previous study, in which such hydrophobic aromatic residues were mostly aggregated, resulting in obvious gel shrinkage[59]. Thus, the remarkable swelling should be attributed to the strong ionic repulsion of the protonated Trp residues. Conversely, when immersed in NaCl aq., the swelling ratios were dramatically lower (1.87 and 1.78 for $x = 3$ and 5, respectively), which is likely due to the mitigation of the ionic repulsion between the protonated Trp residues[60,61]. Interestingly, serious shrinking was observed for the D- and L-Trp(*x*)-gels in Pd(II) aq. instead of expected swelling. The resulting gels were black and solidified, implying the formation of complexes between the Trp residues and Pd(II). This possibility was further examined by ^{1}H-NMR of AC-Trp(L) in D_2O, in which significant peak splits were detected after the addition of Na_2PdCl_4 (Supplementary Fig. 7). Moreover, a large amount of orange precipitate was observed in the clear D_2O solution of AC-Trp(L) when $NaPdCl_4$ was added. These phenomena demonstrated that the gel shrinkage was caused by complexation of Trp residues with Pd(II).

By contrast, the βCD-gel prepared from water swelled slightly in both pure water and aqueous NaCl. As the swelling ratios in water and NaCl aq. were nearly identical, the effect of NaCl on βCD-gel swelling is likely negligible. Conversely, the βCD-gel gradually shrunk and finally became brown in Pd(II) aq. (Supplementary Fig. 8). The shrinkage of the βCD-gel is likely the result of osmotic dehydration with slight Pd(II) accumulation because the gel was still soft and the process was relatively slow, i.e., 1~2 days for the βCD-gel but 2~3 h for the D- or L-Trp(*x*)-gel.

Effect of aqueous solution composition on gel interactions. Gel interaction studies of the D-Trp(5)-gel, L-Trp(5)-gel, and βCD-gel were sequentially performed in pure water, NaCl aq., and Pd(II) aq. First, pieces of the βCD-gel and D- and L-Trp(5)-gels were placed in a glass petri dish with pure water. After agitation, no gel interaction was observed (Fig. 3a; Supplementary Movie 1). By contrast, in NaCl aq., the βCD-gel immediately assembled with both D- and L-Trp(5)-gels without selectivity (Fig. 3b; Supplementary Movie 2). The formed checkered gel aggregate is sufficiently stable to be lifted, indicating strong adhesion between the βCD-gel and the D- and L-Trp(5)-gels. Finally, in Pd(II) aq., no gel interactions were observed (Fig. 3c; Supplementary Movie 3).

These observations indicate that the gel interactions are strongly dependent on the components of the aqueous solutions. In pure water, the D- and L-Trp(5)-gels are largely swollen, which results in extremely low concentrations of the Trp moiety (3.2 mM) (Fig. 2; Supplementary Table 1). Such low concentrations in the D- and L-Trp(5)-gels are not high enough to form sufficient host–guest complexes on the interface of the βCD-gel to bind them together. By contrast, in NaCl aq., the expansion of the D- and L-Trp(5)-gels is well controlled, and the concentrations of Trp residues are appropriately high (55 and 57 mM) and close to the concentration of the βCD residue in the βCD-gel (61 mM). Hence, sufficient host–guest interactions can occur on the interface of the βCD-gel and D- or L-Trp(5)-gels to make them bind strongly. The concentrations of D- and L-Trp residues in the D- and L-Trp(5)-gels and the concentration of βCD residues in the βCD-gel are highest in Pd(II) aq. (170, 198, and 138 mM); thus, the strongest affinities are expected for gel assemblies in that

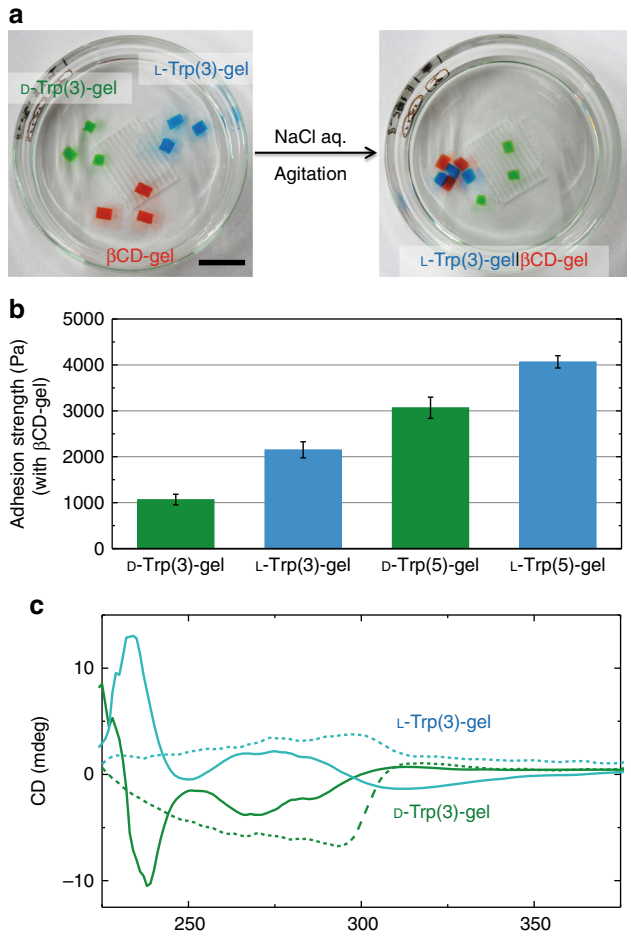

Fig. 4 Macroscopic chiral discrimination of the homochiral D- and L-Trp(3)-gel by the βCD-gel. **a** βCD-gel assembles with the L-Trp(3)-gel but does not interact with the D-Trp(3)-gel in NaCl aq. Scale bar, 1.0 cm. **b** Adhesion strengths for gel assemblies as estimated by stress-strain measurements. Error bars show the standard deviation of measurements for three samples. **c** CD spectra for the D- and L-Trp(3)-gels in water (solid line) and NaCl aq. (dot line), respectively

solution. However, no gel assemblies were formed. This lack of assembly is likely attributed to the aggregation of Trp moieties that formed complexes with Pd(II), which does not involve βCD. Therefore, both the concentration and bound/unbound state of the Trp moieties are fundamental for macroscopic gel assembly in this study.

Visible chiral recognition on a macroscopic scale. To test the possibility of macroscopic chiral recognition, the interactions of the D-Trp(3)-gel and L-Trp(3)-gel with the βCD-gel were investigated in NaCl aq. Interestingly, the βCD-gel assembled with the L-Trp(3)-gel to form an aggregate but did not interact with the D-Trp(3)-gel (Fig. 4a; Supplementary Movie 4). This observation demonstrates that the βCD-gel can enantioselectively differentiate between the D- and L-Trp(3)-gels on a macroscopic scale. Moreover, the binding ability out of NaCl aq. was also examined that the βCD-gel adhered to L-Trp(3)-gel instead of D-Trp(3)-gel after treating with water (Supplementary Fig. 9; Supplementary Movie 5).

Subsequently, rupture stress-strain measurements were carried out to evaluate the adhesion strengths of these gel assemblies. A pair of assembled βCD-gel and D- or L-Trp(x)-gel was removed from the NaCl solution and set on a tensile meter to measure the stress values as strain was applied (Supplementary Fig. 10; Supplementary Movie 6). From the results shown in Fig. 4b, the adhesion strengths for the βCD-gel with the D- and L-Trp(5)-gels show higher values (3070 and 4070 Pa, respectively) than those of the D- and L-Trp(3)-gels (2150 and 1066 Pa, respectively), suggesting that the adhesion strength for the gel assembly is concentration dependent. In the case of the same x, the adhesion of the βCD-gel with the L-Trp(x)-gel is always stronger than that of the D-Trp(x)-gel. Consequently, the adhesion strength for the βCD-gel and D-Trp(3)-gel is the weakest and is not sufficient for forming an assembly in NaCl aq.

To discover the reason for the difference in the interaction of the βCD-gel with the D- and L-Trp(x)-gels, the molecular interactions between βCD and Trp(D) and Trp(L) moieties were investigated using a model system consisting of water-soluble polyacrylamide modified with 1 mol% Trp moiety (pAAm/Trp(D or L), Supplementary Fig. 11). Using fluorescence, the association constant (K_a) values for βCD with residues of Trp(D) and Trp(L) were determined to be 896 and 1890 M^{-1}, respectively (Supplementary Fig. 12). These values are much higher than the reported K_a values for βCD with native Trp(D) and Trp(L) molecules, i.e., 13 and 214 M^{-1} [49]. The higher K_a value for βCD with the Trp(L) moiety suggests that βCD prefers to bind to Trp (L) residues over Trp(D) residues. Thus, the macroscopic enantioselectivity of the βCD-gel for the D- and L-Trp(3)-gels is obviously due to the difference in host–guest molecular association, which is further amplified on the interface of gel assembly through multisite interactions.

Indeed, if the chiral signal has not been correctly transferred to the gel objects, that is, achiral or same chirality for the gels, then the above observation can more precisely be described as macroscopic enantiomeric selectivity than macroscopic chiral discrimination. Fortunately, the circular dichroism (CD) spectra of the D- and L-Trp(3)-gels showed opposite signals both in water and NaCl aq., suggesting that the gels had different homochiralities (Fig. 4c). Accordingly, the CD spectra for the monomers of AC-Trp(D or L) in water and NaCl aq. were also measured, which indicated the influence of NaCl component was almost negligible on CD spectra (Supplementary Fig. 13). In contrast to the curves for the Trp-gels matched well with AC-Trp monomers in water, the spectra for the Trp-gels in NaCl aq. became flatter and reduced gradually near shorter wavelength. This should be caused by the relatively high UV absorbance of Trp-gels in NaCl aq. owing to their higher Trp residue concentrations (Supplementary Figure 14 and 15). However, the signals for the indole group close to the chiral center of the Trp moiety (~280 nm) show similar tendencies for the D- and L-Trp-gels with relative AC-Trp(D) and AC-Trp(L) monomers both in water and NaCl aq., implying the chirality is successfully transferred and amplified in the corresponding gels without conformational chiral interference. This result has two main explanations, which are as follows: (1) the pAAm main-chain is water soluble and flexible enough to avoid helical structural transition, and (2) the ionic repulsion of protonated Trp residues prevents aggregation formation. Therefore, macroscopic chiral discrimination that relies on enantioselective host–guest interactions has been achieved (Fig. 5).

Discussion

Assembly that depends on chiral recognition at various scales is not only crucial for living organisms but also of great importance in artificial systems. In this study, we reported visible chiral recognition via the macroscopic assembly of D-Trp(x)-gel, L-Trp (x)-gel, and βCD-gel. The gel interactions were strongly related to the components of the aqueous solutions, and in aqueous NaCl,

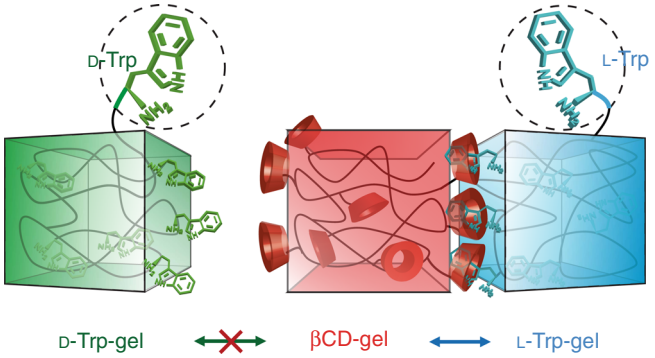

Fig. 5 Conceptual illustration for visible chiral recognition via macroscopic selective assembly. Macroscopic chiral recognition is realized by amplifying enantioselective host–guest associations through interfacial multisite interactions

the βCD-gel successfully differentiated between the D- and L-Trp (3)-gels, which possess opposite chirality through transter from chiral Trp moieties. This achievement was realized due to the amplification of enantioselective host–guest interactions on the interface of the gel assemblies.

Chiral discrimination became visible in this experiment owing to macroscopic selective gel assembly, a process as clear as distinguishing our left and right hands, which originally defined chirality. This visible distinction would be beneficial for improving the understanding of chirality not only for scientists but also for the general public. We believe that the work presented here may contribute to the development of chiral recognition and separation.

Methods

Measurements. ^{1}H NMR spectra were measured using a JEOL JNM-ECA500 spectrometer. Solid–state ^{1}H FG-MAS NMR spectra were recorded on a JEOL ECA-400 spectrometer with a sample spinning rate of 7 kHz. Chemical shifts were referenced to the solvent signals (2.49, 4.79, and 7.26 p.p.m. for DMSO-d_6, D_2O, and $CDCl_3$, respectively). Electrospray ionization mass spectrometry (ESI-MS) were collected on a Thermo Fisher LTQ Orbitrap XL. Fluorescence spectra for solutions of the model systems were obtained on a HITACHI F-2500 spectrophotometer using a 1 cm quartz cuvette ($\lambda_{ex} = 290$ nm). The absorption spectra were measured with a JASCO V-650 spectrometer. Circular dichroism spectra were determined by a JASCO J820 spectrometer. Gel assembly tests were carried out using an EYELA CM-1000 cute mixer. The agitation speed was fixed at ~450 rpm unless otherwise indicated. Stress-strain curves for gel assemblies were recorded using a Yamaden RE-33005 Rheoner creep meter. Each sample was prepared in a quartz mold with a 5×3 mm^2 cross sectional area and measured at a rate of 0.1 mm s^{-1} at room temperature. The swelling ratios were obtained as follow: as-synthesized Trp-gels from DMSO was cut into several samples (V_0), and every three of them were immersed in each solution, i.e., pure water, NaCl aq., and Pd(II) aq., respectively. After 3 days, the volumes of gels in each aqueous solution were determined (V) to give swelling ratios as V/V_0. The βCD-gels were synthesized from water and their swelling ratios were obtained by following the same steps as mentioned above (Fig. 2 and Supplementary Table 1).

Materials. *N*-(*Tert*-butoxycarbonyl)-D-tryptophan (BOC-D-Trp) and *N*-(*tert*-butoxycarbonyl)-L-tryptophan (BOC-L-Trp) were purchased from Tokyo Chemical Industries Co. Ltd., and β-cyclodextrin (βCD) was obtained from Junsei Chemical. All other reagents and solvents were purchased from Nacalai Tesque Inc., Tokyo Chemical Industries Cod. Ltd., Wako Pure Chemical Industries Ltd. or Sigma-Aldrich Co. and used without further purification.

2-Aminoethyl-BOC-D-(or L-)Trp (**1D** or **1L**)) was prepared from BOC-D-(or L-)Trp following the procedures of Tammler et al.[62] (Supplementary Fig. 1).

Synthesis of 2D and 2L. Acryloyl chloride (0.72 g, 8 mmol) in THF (5 mL) was added dropwise to a solution of **1D** (or **1L**) (1.4 g, 4 mmol) and triethylamine (TEA) (0.81 g, 8 mmol) in THF (35 mL) at 0 °C. The mixture was allowed to react for 1 h at 0 °C and then overnight at room temperature. The solution was concentrated and purified by silica gel chromatography to give the product **2D** (or **2L**) in 54 % yield (Supplementary Figure 1). See Supplementary Fig. 2 and 3 for ^{1}H NMR spectra.

Synthesis of acrylamido D- or L-Trp (AC-Trp(D or L)). Trifluoroacetic acid (TFA) (1 mL, 13 mmol) was added dropwise to a solution of **2D** (or **2L**) (200 mg, 0.5 mmol) in DCM (1 mL) at 0 °C. The mixture was stirred for 1 h at 0 °C and an additional 1 h at room temperature. The reaction solution was poured into diethyl ether (50 mL) to generate a precipitate and then vacuum dried to give the final product (Supplementary Fig. 1). Yield 87%. ESI-MS: calcd. for $(C_{16}H_{20}N_4O_2)^+$ = 301.17 ($[M + H]^+$); m/z = 301.17, $[M + Na]^+$ 323.15 for AC-Trp(D); $[M + Na]^+$ 323.17, $[M + K]^+$ 339.17 for AC-Trp(L). See Supplementary Figure 2 and 3 for ^{1}H NMR spectra.

Preparation of the D- or L-Trp(x)-gel. A predetermined amount of acrylamide (AAm), *N*,*N*'-methylenebis(acrylamide) (MBA), and AC-TAm(D or L) were dissolved in DMSO (3.0 mL, total monomer concentration: 6.0 M). After purging with dry argon for 30 min, Irgacure 184 (1.0 mol%) was added to the monomer solution. The reaction mixture was placed in a 1 cm quartz cuvette and sealed. The cuvette was irradiated with UV light at room temperature for 3 h. The newly formed gel was washed with DMSO and excess water to remove traces of initiator and unreacted monomers.

Preparation of the model polymer of pAAm/Trp(D or L). Predetermined amounts of AAm and AC-Trp(D or L) were dissolved in DMSO. After dry argon was used to purge the solution for 30 min, APS (1.0 mol%) was added to the monomer solution. The reaction mixture was placed in a cuvette equipped with a stirrer, and the cuvette was sealed. The cuvette was then warmed in an oil bath thermostated at 65 °C overnight. The reaction mixture was poured into excess methanol to give a precipitate. The newly formed polymer was recovered by filtration and dried under vacuum. See Supplementary Figure 11.

Data availability. All data are available from the authors upon reasonable request.

Received: 19 September 2017 Accepted: 5 December 2017
Published online: 08 March 2018

References

1. Morrow, S. M., Bissette, A. J. & Fletcher, S. P. Transmission of chirality through space and across length scales. *Nat. Nanotechnol.* **12**, 410–419 (2017).
2. Qing, G. & Sun, T. The transformation of chiral signals into macroscopic properties of materials using chirality-responsive polymers. *NPG Asia Mater.* **4**, e4 (2012).
3. Shimomura, K., Ikai, T., Kanoh, S., Yashima, E. & Maeda, K. Switchable enantioseparation based on macromolecular memory of a helical polyacetylene in the solid state. *Nat. Chem.* **6**, 429–434 (2014).
4. Hazen, R. M. & Sholl, D. S. Chiral selection on inorganic crystalline surfaces. *Nat. Mater.* **2**, 367–374 (2003).
5. Roche, C. et al. Homochorial columns constructed by chiral self-sorting during supramolecular helical organization of hat-shaped molecules. *J. Am. Chem. Soc.* **136**, 7169–7185 (2014).
6. Liang, J., Wu, Y., Deng, X. & Deng, J. Optically active porous materials constructed by chirally helical substituted polyacetylene through a high internal phase emulsion approach and the application in enantioselective crystallization. *ACS Macro Lett.* **4**, 1179–1183 (2015).
7. Irie, M., Fukaminato, T., Matsuda, K. & Kobatake, S. Photochromism of diarylethene molecules and crystals: memories, switches, and actuators. *Chem. Rev.* **114**, 12174–12277 (2014).
8. Li, W. et al. Enantiospecific photoresponse of sterically hindered diarylethenes for chiroptical switches and photomemories. *Sci. Rep.* **5**, 9186 (2015).
9. Miao, W., Wang, S. & Liu, M. Reversible quadruple switching with optical, chiroptical, helicity, and macropattern in self-assembled spiropyran gels. *Adv. Funct. Mater.* https://doi.org/10.1002/adfm.201701368 (2017).
10. Shopsowitz, K. E., Qi, H., Hamad, W. Y. & MacLachlan, M. J. Free-standing mesoporous silica films with tunable chiral nematic structures. *Nature* **468**, 422–426 (2010).
11. Torsi, L. et al. A sensitivity-enhanced field-effect chiral sensor. *Nat. Mater.* **7**, 412–417 (2008).
12. Iamsaard, S. et al. Conversion of light into macroscopic helical motion. *Nat. Chem.* **6**, 229–235 (2014).

13. Panda, M. K., Runčevski, T., Husain, A., Dinnebier, R. E. & Naumov, P. Perpetually self-propelling chiral single crystals. *J. Am. Chem. Soc.* **137**, 1895–1902 (2015).
14. Pieraccini, S., Masiero, S., Ferrarini, A. & Spada, G. P. Chirality transfer across length-scales in nematic liquid crystals: fundamentals and applications. *Chem. Soc. Rev.* **40**, 258–271 (2011).
15. Liu, M., Zhang, L. & Wang, T. Supramolecular chirality in self-assembled systems. *Chem. Rev.* **115**, 7304–7397 (2015).
16. Yashima, E. et al. Supramolecular helical systems: helical assemblies of small molecules, foldamers, and polymers with chiral amplification and their functions. *Chem. Rev.* **116**, 13752–13990 (2016).
17. Mattia, E. & Otto, S. Supramolecular systems chemistry. *Nat. Nanotechnol.* **10**, 111–119 (2015).
18. Yashima, E., Maeda, K., Iida, H., Furusho, Y. & Nagai, K. Helical polymers: synthesis, structures, and functions. *Chem. Rev.* **109**, 6102–6211 (2009).
19. Ho, R.-M., Wang, H.–F. & Li, M.–C. in *Encyclopedia of Polymer Science and Technology* 1–33 (John Wiley & Sons, Inc., 2014).
20. de Bruin, A. G., Barbour, M. E. & Briscoe, W. H. Macromolecular and supramolecular chirality: a twist in the polymer tales. *Polym. Int.* **63**, 165–171 (2013).
21. Roche, C. et al. A supramolecular helix that disregards chirality. *Nat. Chem.* **8**, 80–89 (2016).
22. Wen, T., Wang, H. –F., Li, M. –C. & Ho, R. –M. Homochiral evolution in self-assembled chiral polymers and block copolymers. *Acc. Chem. Res.* **50**, 1011–1021 (2017).
23. Huang, Z. et al. Pulsating tubules from noncovalent macrocycles. *Science* **337**, 1521–1526 (2012).
24. Korevaar, P. A. et al. Pathway complexity in supramolecular polymerization. *Nature* **481**, 492–496 (2012).
25. Kim, J. et al. Induction and control of supramolecular chirality by light in self-assembled helical nanostructures. *Nat. Commun.* **6**, 6959 (2015).
26. Zhang, M. & Ye, B. –C. Colorimetric chiral recognition of enantiomers using the nucleotide-capped silver nanoparticles. *Anal. Chem.* **83**, 1504–1509 (2011).
27. Yashima, E., Maeda, K. & Sato, O. Switching of a macromolecular helicity for visual distinction of molecular recognition events. *J. Am. Chem. Soc.* **123**, 8159–8160 (2001).
28. Tsubaki, K. et al. Visual enantiomeric recognition using chiral phenolphthalein derivatives. *Org. Lett.* **3**, 4071–4073 (2001).
29. Wang, C. et al. Enantioselective fluorescent recognition in the fluorous phase: enhanced reactivity and expanded chiral recognition. *J. Am. Chem. Soc.* **137**, 3747–3750 (2015).
30. Xiong, J. –B. et al. Enantioselective recognition for many different kinds of chiral guests by one chiral receptor based on tetraphenylethylene cyclohexylbisurea. *J. Org. Chem.* **81**, 3720–3726 (2016).
31. Miao, W., Zhang, L., Wang, X., Qin, L. & Liu, M. Gelation-induced visible supramolecular chiral recognition by fluorescent metal complexes of quinolinol-glutamide. *Langmuir* **29**, 5435–5442 (2013).
32. Wen, T. et al. Controlled handedness of twisted lamellae in banded spherulites of isotactic poly(2-vinylpyridine) as induced by chiral dopants. *Angew. Chem. Int. Ed.* **54**, 14313–14316 (2015).
33. Oaki, Y. & Imai, H. Amplification of chirality from molecules into morphology of crystals through molecular recognition. *J. Am. Chem. Soc.* **126**, 9271–9275 (2004).
34. Maeda, K., Mochizuki, H., Osato, K. & Yashima, E. Stimuli-responsive helical poly(phenylacetylene)s bearing cyclodextrin pendants that exhibit enantioselective gelation in response to chirality of a chiral amine and hierarchical super-structured helix formation. *Macromolecules* **44**, 3217–3226 (2011).
35. Chen, X. et al. Enantioselective gel collapsing: a new means of visual chiral sensing. *J. Am. Chem. Soc.* **132**, 7297–7299 (2010).
36. Tu, T., Fang, W., Bao, X., Li, X. & Dötz, K. H. Visual chiral recognition through enantioselective metallogel collapsing: synthesis, characterization, and application of platinum-steroid low-molecular-mass gelators. *Angew. Chem. Int. Ed.* **50**, 6601–6605 (2011).
37. Qing, G. & Sun, T. Chirality-driven wettability switching and mass transfer. *Angew. Chem. Int. Ed.* **53**, 930–932 (2013).
38. Shundo, A., Hori, K., Ikeda, T., Kimizuka, N. & Tanaka, K. Design of a dynamic polymer interface for chiral discrimination. *J. Am. Chem. Soc.* **135**, 10282–10285 (2013).
39. Ding, S., Cao, S., Zhu, A. & Shi, G. Wettability switching of electrode for signal amplification: conversion of conformational change of stimuli-responsive polymer into enhanced electrochemical chiral analysis. *Anal. Chem.* **88**, 12219–12226 (2016).
40. Tang, W., Ng, S. –C. & Sun, D. *Modified Cyclodextrins for Chiral Separation*. (Springer-Verlag, Berlin Heidelberg, 2013).
41. Kida, T., Iwamoto, T., Asahara, H., Hinoue, T. & Akashi, M. Chiral recognition and kinetic resolution of aromatic amines via supramolecular chiral nanocapsules in nonpolar solvents. *J. Am. Chem. Soc.* **135**, 3371–3374 (2013).
42. Gingter, S., Bezdushna, E. & Ritter, H. Chiral recognition of macromolecules with cyclodextrins: pH- and thermosensitive copolymers from *N*-isopropylacrylamide and *N*-acryloyl-D/L-phenylalanine and their inclusion complexes with cyclodextrins. *Beilstein. J. Org. Chem.* **7**, 204–209 (2011).
43. Liang, J., Song, C. & Deng, J. Optically active microspheres constructed by helical substituted polyacetylene and used for adsorption of organic compounds in aqueous systems. *ACS Appl. Mater. Interfaces* **6**, 19041–19049 (2014).
44. Han, C. et al. Enantioselective recognition in biomimetic single artificial nanochannels. *J. Am. Chem. Soc.* **133**, 7644–7647 (2011).
45. Tao, Y., Dai, J., Kong, Y. & Sha, Y. Temperature-sensitive electrochemical recognition of tryptophan enantiomers based on β-cyclodextrin self-assembled on poly (L-glutamic acid). *Anal. Chem.* **86**, 2633–2639 (2014).
46. Han, S. M. Direct enantiomeric separations by high performance liquid chromatography using cyclodextrins. *Biomed. Chromatogr.* **11**, 259–271 (1997).
47. Kepert, I. et al. D-tryptophan from probiotic bacteria influences the gut microbiome and allergic airway disease. *J. Allergy Clin. Immunol.* **139**, 1525–1535 (2017).
48. Shimazaki, Y., Yajima, T., Takani, M. & Yamauchi, O. Metal complexes involving indole rings: structures and effects of metal-indole interactions. *Coord. Chem. Rev.* **253**, 479–492 (2009).
49. Rekharsky, M. V. & Inoue, Y. Complexation thermodynamics of cyclodextrins. *Chem. Rev.* **98**, 1875–1917 (1998).
50. Xie, G. et al. Chiral recognition of L-tryptophan with beta-cyclodextrin-modified biomimetic single nanochannel. *Chem. Commun.* **51**, 3135–3138 (2015).
51. Harada, A., Kobayashi, R., Takashima, T., Hashidzume, A. & Yamaguchi, H. Macroscopic self-assembly through molecular recognition. *Nat. Chem.* **3**, 34–37 (2011).
52. Yamaguchi, H. et al. Photoswitchable gel assembly based on molecular recognition. *Nat. Commun.* **3**, 603 (2012).
53. Zheng, Y., Hashidzume, A., Takashima, Y., Yamaguchi, H. & Harada, A. Switching of macroscopic molecular recognition selectivity using a mixed solvent system. *Nat. Commun.* **3**, 831 (2012).
54. Nakamura, T., Takashima, Y., Hashidzume, A., Yamaguchi, H. & Harada, A. A metal-ion-responsive adhesive material via switching of molecular recognition properties. *Nat. Commun.* **5**, 4622 (2014).
55. Nakahata, M., Takashima, Y. & Harada, A. Redox-responsive macroscopic gel assembly based on discrete dual interactions. *Angew. Chem. Int. Ed.* **53**, 3617–3621 (2014).
56. Zheng, Y., Hashidzume, A., Takashima, T., Yamaguchi, H. & Harada, A. Macroscopic observations of molecular recognition: discrimination of the substituted position on the naphthyl group by polyacrylamide gel modified with β-cyclodextrin. *Langmuir* **27**, 13790–13795 (2011).
57. Zheng, Y., Hashidzume, A., Takashima, T., Yamaguchi, H. & Harada, A. Temperature-sensitive macroscopic assembly based on molecular recognition. *ACS Macro Lett.* **1**, 1083–1085 (2012).
58. Zheng, Y., Hashidzume, A. & Harada, A. pH-Responsive self-assembly by molecular recognition on a macroscopic scale. *Macromol. Rapid Commun.* **34**, 1062–1066 (2013).
59. Hashidzume, A., Zheng, Y., Takashima, T., Yamaguchi, H. & Harada, A. Macroscopic self-assembly based on molecular recognition: effect of linkage between aromatics and the polyacrylamide gel scaffold, amide versus ester. *Macromolecules* **46**, 1939–1947 (2013).
60. Zhao, Y., Su, H., Fang, L. & Tan, T. Superabsorbent hydrogels from poly (aspartic acid) with salt-, temperature- and pH-responsiveness properties. *Polymer* **46**, 5368–5376 (2005).
61. Kabiri, K., Omidian, H., Hashemi, S. A. & Zohuriaan-Mehr, M. J. Synthesis of fast-swelling superabsorbent hydrogels: effect of crosslinker type and concentration on porosity and absorption rate. *Eur. Polym. J.* **39**, 1341–1348 (2003).
62. Tammler, U., Quillan, J. M., Lehmann, J., Sadée, W. & Kassack, M. U. Design, synthesis, and biological evaluation of non-peptidic ligands at the Xenopus laevis skin-melanocortin receptor. *Eur. J. Med. Chem.* **38**, 481–493 (2003).

Acknowledgements

This work was supported by the ImPACT Program of Council for Science, Technology, and Innovation (Cabinet Office, Government of Japan). The authors thank Dr. Naoya Inazumi (Osaka University) for the NMR measurements and Mr. Takuma Adachi (Osaka University) for assistance with the CD spectrum measurements.

Author contributions

Y.Z. and A.Har: Conceived the project. Y.Z.: Designed and prepared all compounds and performed all the experiments. A.Has., Y.T., and H.Y.: Advised on the data analysis. Y.K.

and T.S.: Assisted with the experiments. Y.Z. and A.Har. Co-wrote the paper. All the authors discussed the results and commented on the manuscript.

Additional information

Supplementary information is available for this paper at https://doi.org/10.1038/s42004-017-0003-x.

Competing interests: The authors declare no competing financial interests.

Reprints and permission information is available online at http://npg.nature.com/reprintsandpermissions/

Publisher's note: Springer Nature remains neutral with regard to jurisdictional claims in published maps and institutional affiliations.